



On adaptive time stepping for large-scale parabolic problems: Computer simulation of heat and mass transfer in vacuum freeze-drying

K. Georgiev^{a,*}, N. Kosturski^a, S. Margenov^a, J. Starý^b

^a Institute for Parallel Processing, Bulgarian Academy of Sciences, Acad. G. Bonchev str., Bl. 25-A, 1113 Sofia, Bulgaria

^b Institute of Geonics, Academy of Sciences of the Czech Republic, Studentská 1768, 708 00 Ostrava - Poruba, Czech Republic

ARTICLE INFO

MSC:
65M60

Keywords:

Vacuum freeze drying
Zeolites
Heat and mass transfer
Parabolic PDE
Finite element method
MIC(0) preconditioning

ABSTRACT

The work is motivated by the problem of freeze-drying, which is a process of dehydrating frozen materials by sublimation under high vacuum. In particular, it concerns the mathematical modelling and computer simulation of the heat and mass transfer with the core in solving the time-dependent nonlinear partial differential equation of parabolic type.

Instead of a uniform discretization of the considered time interval, an adaptive time-stepping procedure is applied in an effort to optimize the whole simulation. The procedure is based on the local comparison of the Crank–Nicolson and backward Euler approximations. The results of numerical experiments performed on a selected real-life problem are included.

© 2008 Elsevier B.V. All rights reserved.

1. Introduction

Freeze-drying is a special technology of dehydrating frozen materials by sublimation under high vacuum [9,6]. One of its possible applications comes from the food industry, where it can be used for drying certain kinds of food-stuffs, for example carrots or coffee.

The apparatus consists of two interconnected containers; see Fig. 1. One is the food camera intended for the product to be dried (it can be seen in the left-hand side of the picture) and the other is the adsorbent camera filled by natural or artificial zeolite granules [12]. There could be one or more adsorption cameras. In Fig. 1 the case with two adsorption cameras is given. Zeolites are a special type of silica-containing material, with a porous structure, applicable as adsorbents and catalysts [1]. Here, they are used for the sorption of water molecules coming through the pipe from the food camera.

The whole process of drying has three phases. The first one is a preparation of the source material in the food container, which is then vacuumed. Also during this phase, the adsorbent located in the second container is activated, which means warmed up, vacuumed and cooled to a room temperature. The second phase is the self-freezing of the source material (after opening the valve between the food and adsorption cameras) surrounded by high vacuum. The last phase is the drying in conditions of an uniform sublimation of water steam from the source material in the food container and its disposal in the adsorbent.

The sublimation is supported by heaters installed in the food camera. The heat is supplied to the source material by conduction, by radiation or by a combination of both methods, but at a proper rate to avoid local melting.

Such kind of drying technology has several advantages. For example, it results in a higher food quality due to the minimum loss of flavour and aroma, and minimal chances of microbial growth due to the absence of water, or no thermal and oxidizing processes.

* Corresponding author.

E-mail address: georgiev@parallel.bas.bg (K. Georgiev).

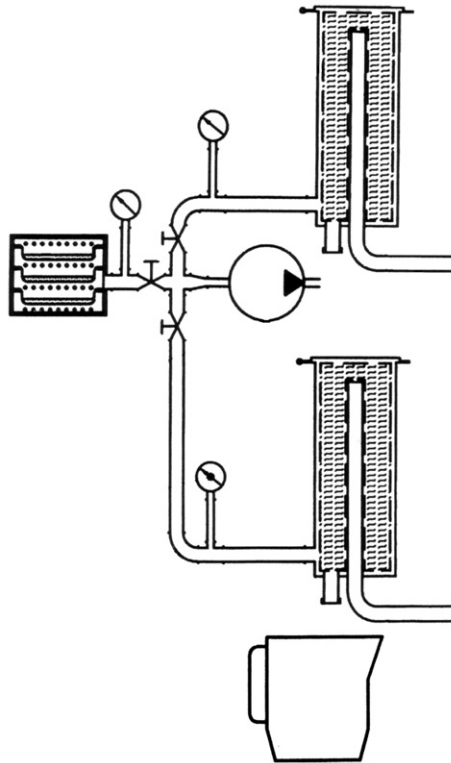


Fig. 1. The apparatus for vacuum freeze-drying.

The mathematical model of the whole process of freeze-drying is described by a system of time-dependent differential equations, but with the possibility to split the processes in the food container and in the adsorbent camera according to the technological subprocesses involved.

2. Heat and mass transfer problem

Further, we will consider only the process of heat and mass transfer in the adsorbent camera. It is described by the nonlinear partial differential equation of parabolic type,

$$c\rho \frac{\partial T}{\partial t} = \mathcal{L}T + f(x, t), \quad x \in \Omega, \quad t > 0, \tag{1}$$

where

$$\mathcal{L}T = \sum_{i=1}^d \frac{\partial}{\partial x_i} \left(k(x, t) \frac{\partial T}{\partial x_i} \right)$$

and $T(x, t)$ denotes the unknown temperature distribution, $k = k(x, t) > 0$ the heat conductivity, $c = c(x, t) > 0$ the heat capacity, and $\rho > 0$ the material density. The function $f(x, t, T)$ is responsible for the process of transfer of water molecules in the adsorption container. By default, d is the given dimension of the space ($d = 2$) and $\Omega \in R^d$ denotes the computational domain.

To the parabolic equation, we assign the initial and boundary conditions in the standard form,

$$\begin{aligned} T(x, 0) &= T_0(x), \quad x \in \Omega, \\ T(x, t) &= \mu(x, t), \quad x \in \Gamma \equiv \partial\Omega, \quad t > 0, \end{aligned}$$

where $T_0(x)$ is the initial temperature distribution in the computational domain, most often the room temperature surrounding the adsorbent camera, and $\mu(x, t)$ is the room temperature during the freeze-drying process, which can be controlled by cooling/heating devices.

The Finite Element Method (FEM) with linear triangle elements (so-called Courant linear finite elements) is applied for discretization in the space of (1) (see e.g. [2]). Let \mathcal{T}_h be a triangulation of the computational domain Ω with discretization

```

for  $k = 1, 2, \dots$  until stop:
  find  $T^k: (M + \tau^k K) T^k = M T^{k-1} + \tau^k F^k$ 
  compute  $r^k = (M + \frac{1}{2} \tau^k K) T^k - (M - \frac{1}{2} \tau^k K) T^{k-1} - \frac{1}{2} \tau^k F^k - \frac{1}{2} \tau^k F^{k-1}$ 
  compute  $\eta^k = \|r^k\| / \|T^k\|$ 
  decide if  $\eta^k < \varepsilon_{\min}$  then  $\tau^{k+1} = 2\tau^k$ 
         if  $\eta^k > \varepsilon_{\max}$  then  $\tau^{k+1} = \tau^k / 2$ 
         if  $\eta^k \in (\varepsilon_{\min}, \varepsilon_{\max})$  or ( $\eta^k < \varepsilon_{\min}$  and  $\eta^{k-1} > \varepsilon_{\max}$ ) then
            $\tau^{k+1} = \tau^k$  and  $T^{k+1} = T^k$ , stop
         if  $\eta^k > \varepsilon_{\max}$  and  $\eta^{k-1} < \varepsilon_{\min}$  then
            $\tau^{k+1} = \tau^k / 2$  and  $T^{k+1} = T^{k-1}$ , stop
end for

```

Fig. 2. The algorithm of the adaptive time-stepping procedure.

parameter h and $\phi = \{\phi_i\}_{i=1}^{N_{sp}}$ be the Lagrangian basis of the finite element space according to the triangulation \mathcal{T}_h . Then, the problem can be written in the following matrix form:

$$M \frac{dT}{dt} + KT = F \quad (2)$$

with the mass matrix M , the stiffness matrix K and the right-hand side F given by the following three expressions:

$$M = \left[\int_{\Omega} c \rho \phi_i \phi_j dx \right]_{i,j=1}^{N_{sp}}, \quad K = \left[\int_{\Omega} k \nabla \phi_i \nabla \phi_j dx \right]_{i,j=1}^{N_{sp}}, \quad F = \left[\int_{\Omega} f(x, t) \phi_i dx \right]_{i=1}^{N_{sp}}.$$

The initial-boundary value problem of heat and mass transfer (2) is discretized by the finite differences in time [2]. Using the simplest finite differences, this leads to the computation of the vector T^k of nodal temperatures at the time levels t_k , $k = 1, \dots, N$, with the time steps $\tau_k = t_k - t_{k-1}$. In the case of a uniform time discretization with a constant time step τ , we solve the linear system

$$(M + \tau \vartheta K) T^k = (M - \tau (1 - \vartheta) K) T^{k-1} + \tau \vartheta F^k + \tau (1 - \vartheta) F^{k-1}. \quad (3)$$

The parameter $\vartheta \in [0, 1]$ sets the time scheme of the computation. We aim to develop a fully robust and stable method; therefore, we restrict our attention to implicit methods with $\vartheta = \frac{1}{2}$ and $\vartheta = 1$, which correspond to the Crank–Nicolson (CN) method and the backward Euler (BE) method [3,8], respectively. In practice, we use the backward Euler method, which is unconditionally stable.

For the solution of the linear system (3) the well-known Conjugate Gradient Method (CGM) with a Modified Incomplete Cholesky factorization (MIC(0)) preconditioner [4,5] is used.

3. Adaptive time steps

To ensure accuracy and not waste computational effort, it is important to adapt the time steps to the behaviour of the solution. In the simplest case, we can test the time change of the solution and change the time step size, if the variation is too small or too large.

A suitable adaptive time-stepping procedure is based on a local comparison of the backward Euler (T_{BE}) and Crank–Nicolson (T_{CN}) approximations and controlled with the aid of the ratio $\eta = \|T_{CN} - T_{BE}\| / \|T_{BE}\|$. However, such an approach requires the solution of two linear systems to obtain T_{BE} and T_{CN} , which is, from the computational point of view, too expensive.

To make it cheaper, we solve only the linear system for the backward Euler steps. We get T_{BE} and can approximate the solution of the corresponding linear system for the Crank–Nicolson steps T_{CN} with $\bar{T}_{CN} \simeq T_{BE} - r$. The residual r arises from the substitution of T_{BE} in the linear system for the Crank–Nicolson steps. In other words, to obtain \bar{T}_{CN} , we perform only Richardson iteration of the linear system for the Crank–Nicolson steps, whereas the initial approximation of the solution is set to be T_{BE} . And consequently, $\eta^k = \|r^k\| / \|T_{BE}^k\|$. The method described below gives the basis of the algorithm for the adaptive time-stepping procedure, see Fig. 2, which was first applied to the mathematical modelling of processes in spent nuclear fuel repositories [10].

The algorithm depends on the choice of the parameters ε_{\min} and ε_{\max} , which should be fit to the problem to be solved. In usual practice, we set $\varepsilon_{\min} = 10^{-8}$ and $\varepsilon_{\max} = 10^{-7}$; see Section 4.3.

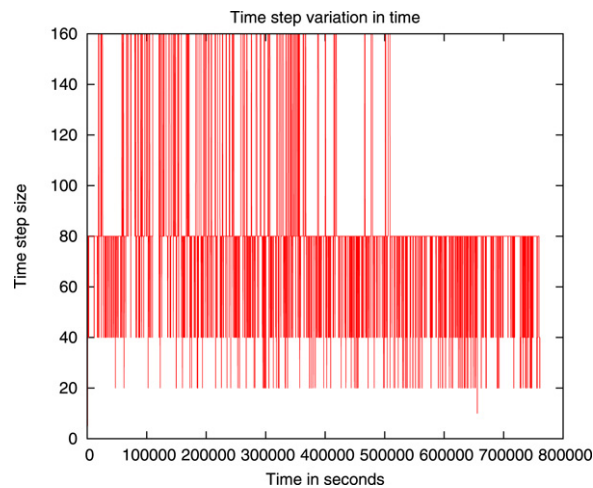


Fig. 3. The time-step change during the execution of one of the test experiments.

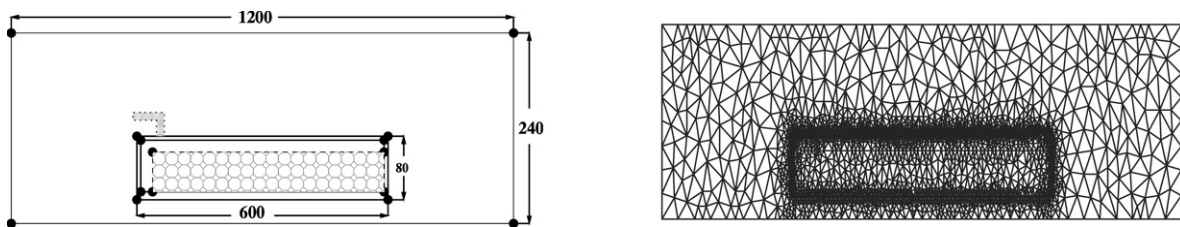


Fig. 4. Model of half of the adsorbent camera and its FE discretization.

The matrix changes in each time step. Therefore, it is advantageous to adapt the time step less frequently and use the adaptively obtained value of τ^k several times. This number of non-adaptive steps #NA, between two following adaptive ones, is the next parameter of the algorithm. We practically use #NA = 4; see Section 4.2. The plot of the varied adaptive time steps corresponding to a simple run can be seen in Fig. 3. The starting value of the time-step τ is chosen as 5 s. During the adaptive procedure it becomes many times greater, but more often it is between 40 and 80 s, i.e. between 8 and 16 times greater than the initial one.

The efficiency of the algorithm can also be increased by using a suitable initial approximation for solving the linear system. For example, the initial approximation can be taken directly from the previous time step, or given by the linear extrapolation of two previous time steps.

4. Numerical experiments

We studied the heat and mass transfer in the adsorption camera by solving the introduced initial-boundary value problem. The numerical methods described were implemented in C++ and the resulting program code was tested on a selected real-life problem. The experiments were performed on a standard PC equipped with a Pentium IV/1.5 GHz processor, 256 kB of L2 cache, 256 MB of memory, and running the Scientific Linux 4.5 operating system.

4.1. Model of the adsorbent camera

For the numerical experiments, we chose the 2D model of the adsorbent camera, which is a part of the technological device for vacuum freeze-drying of grated carrots. Due to the symmetry, the model includes only one half of the container, surrounded by the room atmosphere. The scheme of the situation is shown in Fig. 4. The container consists of three subdomains: the walls of the container, the vacuum zone, and the area with zeolite granules.

The computational domain is discretized by linear triangular finite elements with the aid of the computer mesh generator Triangle [7,11]. For the generation, the options for a minimal angle of a triangle (the most often used value is 30°) and for a minimal area of a single triangle (depending on different subdomains and on the geometry) were applied. The mesh is refined around the walls of the container, resulting in 6568 nodes and 12 819 elements.

The time interval considered varies for testing purposes and for the computations of the full modeling sequence. The first is done for 5000 s, whilst the time interval for the second is set to be 760 405 s, which means more than 8 days and 19 h.

Table 1

Test results for the various #NA

#NA	Time (s)	#It	#It _A	#TS	τ^*	$\frac{\ T - T_{\text{ex}}\ _2}{\ T\ _2}$	$\ T - T_{\text{ex}}\ _{\infty}$
0	28.47	8515	8515	104	48.1	3.87×10^{-6}	1.53×10^{-3}
2	20.40	6700	3110	88	56.8	4.68×10^{-6}	1.88×10^{-3}
4	15.89	5540	1513	77	64.9	3.31×10^{-6}	1.36×10^{-3}
8	18.19	6225	1204	95	52.6	5.55×10^{-6}	2.32×10^{-3}
16	17.66	6073	664	99	50.5	5.55×10^{-6}	2.32×10^{-3}
32	16.37	5661	366	93	53.8	4.35×10^{-6}	1.80×10^{-3}

Constant time steps $\tau = 5$ s: Time = 109.07 s, #It = 33 067, #TS = 999.**Table 2**Test result for the various combinations of ε_{\min} and ε_{\max}

ε_{\min}	ε_{\max}	Time (s)	#It	#It _A	#TS	τ^*	$\frac{\ T - T_{\text{ex}}\ _2}{\ T\ _2}$	$\ T - T_{\text{ex}}\ _{\infty}$
10^{-9}	10^{-8}	38.33	11 869	2996	265	19	2.17×10^{-6}	8.18×10^{-4}
10^{-8}	10^{-7}	15.89	5 540	1513	77	65	3.31×10^{-6}	1.36×10^{-3}
10^{-7}	10^{-6}	9.27	3 321	929	37	135	8.66×10^{-6}	4.08×10^{-3}
10^{-6}	10^{-5}	3.71	1 291	699	7	714	2.86×10^{-5}	2.29×10^{-2}

Constant time steps $\tau = 5$ s: Time = 109.07 s, #It = 33 067, #TS = 999.

The adaptive time-stepping procedure always begins with $\tau = 5$ s. In each time step, we solve the linear system by the preconditioned conjugate gradient method up to the relative residual accuracy $\varepsilon_{\text{PCG}} = 10^{-9}$.

4.2. How often is it necessary to perform the adaptive time stepping procedure?

The first tests of the solver were aimed at discovering the optimal number of times to perform the adaptive time stepping procedure, and to fit the parameter #NA to the studied problem. For the various values #NA, we solved the model problem in the shorter time interval, whilst the other parameters were fixed, $\varepsilon_{\min} = 10^{-8}$ and $\varepsilon_{\max} = 10^{-7}$; see Table 1.

Instead of varying #NA, the table includes the measured wall-clock time of the computation, and further, the number of all PCG iterations #It; separately, also the number of PCG iterations performed only during the adaptive time steps #It_A, the number of time steps necessary for the considered time interval #TS, the averaged time step τ^* , and the errors of the solution. Here, the exact solution vector T_{ex} means the solution of the problem for the constant time steps $\tau = 5$ s by the Crank–Nicolson method.

The results confirm the usefulness of the adaptive time steps. In comparison with computation involving only the uniform time discretization, the measured wall-clock time is shorter by more than 5 times, the number of required time steps #TS is less by more than 10 times, and the number of necessary PCG iterations #It by more than 4 times. The errors stay almost constant and independent of the choice of #NA.

Therefore, we recommend #NA $\in [2, 16]$ with the preference of smaller values to approximate the time evolution of the problem more precisely and not to miss possible stronger gradients of the solution. Practically, we choose #NA = 4.

4.3. How to set the other parameters

During the numerical experiments involving the shorter time interval, we tried also to fit the parameters ε_{\min} and ε_{\max} to the solved problem, whilst the number of non-adaptive steps stayed fixed, #NA = 4; see Table 2.

The obtained results demonstrate the sensitivity of the computation on the choice of the parameters ε_{\min} and ε_{\max} , which influences the resulting number of PCG iterations #It, the number of time steps #TS, and thus also the measured computation time. Moreover, they affect the errors of the numerical solution.

In the case of our application and for the given relative accuracy of the PCG iterations ε_{PCG} , the considered values of ε_{\min} and ε_{\max} should be bounded to $\varepsilon_{\min} \in \langle \varepsilon_{\text{PCG}}, \varepsilon_{\text{PCG}} \cdot 10^2 \rangle$ and $\varepsilon_{\max} = \varepsilon_{\min} \cdot 10$.

4.4. Impact on computer simulations of the whole drying cycle

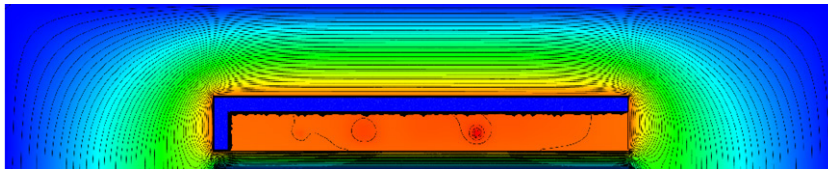
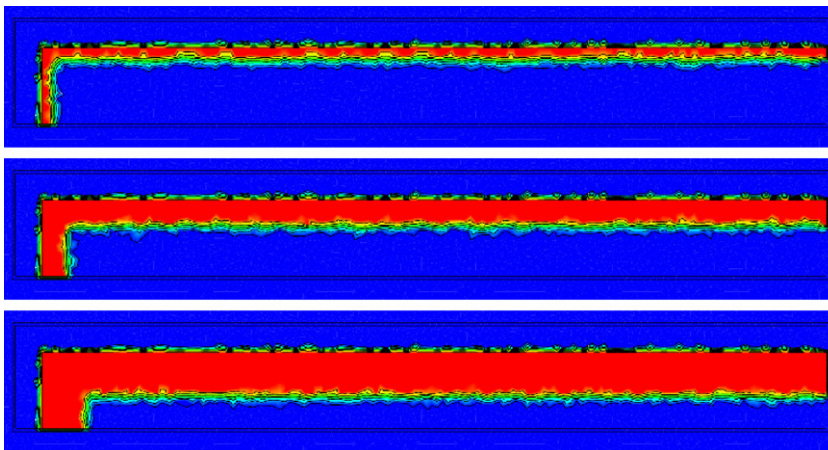
To get a better idea about the practical efficiency of the adaptive time-stepping procedure in vacuum freeze-drying computer simulation, we also performed numerical tests in the full time interval, set to be more than 8 days and 19 h; see Table 3. In accordance with the previous results, we tested three combinations of the input parameters ε_{\min} and ε_{\max} together with a fixed number of non-adaptive time steps, #NA = 4.

Applying the uniform time discretization, the large-scale computation requires more than 152 thousand time steps, consuming 4 h and 41 min of the computer power. However, due to the relatively smooth and go-easy process of heat and mass transfer, it is not necessary to perform so many very small time steps. In this respect, the adaptive time-stepping procedure helps to optimize the computer simulation. According to the chosen input parameters ε_{\min} and ε_{\max} ,

Table 3

The results of the full time interval computations

ε_{\min}	ε_{\max}	Time (s)	#It	#TS	τ^*	$\frac{\ T - T_{\text{ex}}\ _2}{\ T\ _2}$	$\ T - T_{\text{ex}}\ _{\infty}$
10^{-9}	10^{-8}	5539.4	1 711 902	35 880	21	1.86×10^{-6}	4.13×10^{-4}
10^{-8}	10^{-7}	2274.6	786 912	10 358	73	6.09×10^{-5}	1.85×10^{-2}
10^{-7}	10^{-6}	800.6	300 058	2 943	258	1.19×10^{-4}	2.29×10^{-2}

The constant time steps $\tau = 5$ s, Time = 16 882.6 s, #It = 5 023 738, #TS = 152 082.**Fig. 5.** The temperature field at the end of the full time interval.**Fig. 6.** The gradual water filling of the zeolite granules.

the computation lasts from 13 min to 1 h and 32 min. Taking into account the acceptable errors of the computation, the full time interval simulation requires 38 min for more than 10 thousand time steps, when $\tau^* = 73$ s.

Let us note, that the adaptive time stepping is strongly varying and non-monotonic (see Fig. 3), which reflects the complex nonlinear nature of the physical process studied.

4.5. From the engineering point of view

The main output of the vacuum freeze-drying computer simulation in the adsorbent camera is the temperature field, see Fig. 5, because the temperature nonlinearly influences the ability of the zeolite granules to adsorb the water steam.

After the activation, the zeolites start to adsorb the water molecules and their water filling accumulates in time, see Fig. 6, including the situation at the first, second and last thirds of the time interval. Due to the water accumulation, the temperature of the zeolites increases and their adsorbent capacity declines. This could lead to the worst-case scenario, when a too high temperature of the zeolites stops or even reverses the adsorption process. For this reason, it is important to monitor or to control the temperature of the zeolite granules and to balance the process of heat and mass transfer in the adsorbent camera.

5. Conclusion

The paper is devoted to the mathematical modelling and computer simulation of the vacuum freeze-drying process. In particular, it concerns the time evolution of the temperature field in the adsorbent camera as well as the transfer of the sublimed water molecules and their retention in the zeolite granules. The problem, described by a time-dependent nonlinear partial differential equation of parabolic type, leads to the repeated solution of linear systems at different time levels.

The current study is based on an existing computer simulator where only uniform time discretization with constant time steps was used. In an effort to optimize the computation, the adaptive time-stepping procedure was implemented and tuned. The procedure is based on the local comparison of Crank–Nicolson and backward Euler approximations.

Finally, numerical tests were performed on a selected large-scale real-life problem. The tests allowed us to find suitable parameters and showed the practical usefulness of the developed solver for such kind of computer simulations.

Acknowledgment

The work presented was supported by the Bulgarian IST Centre of Competence in 21st Century BIS-21⁺⁺ funded by the European Commission within FP6 INCO through the project 016639/2005.

References

- [1] G. Tsitshvili, T. Andronikashvili, G. Kirov, *Natural Zeolites*, Prentice Hall, 1992.
- [2] S. Brenner, L. Scott, *The Mathematical Theory of Finite Element Methods*, in: *Texts in Applied Mathematics*, vol. 15, Springer-Verlag, 1994.
- [3] A. Quarteroni, A. Valli, *Numerical Approximation of Partial Differential Equations*, in: *SCM Series*, vol. 23, Springer-Verlag, Heidelberg, 1994, p. 543.
- [4] O. Axelsson, *Iterative Solution Methods*, Cambridge University Press, 1996.
- [5] I. Gustafsson, An incomplete factorization preconditioning method based on modification of element matrices, *BIT* 36 (1) (1996) 86–100.
- [6] A. Mujumdar, *Handbook of Industrial Drying*, Marcel Dekker, Inc., 1999.
- [7] P. Frey, P.-L. George, *Mesh Generation*, Hermes Science, 2000.
- [8] D. Kincaid, W. Cheney, *Numerical Analysis: Mathematics of Scientific Computing*, Thomson Learning, 2002.
- [9] F. Jafar, M. Farid, Analysis of heat and mass transfer in freeze-drying, *Drying Technology* 21 (2) (2003) 249–263.
- [10] R. Blaheta, P. Byczanski, R. Kohut, J. Starý, Algorithms for parallel FEM modelling of thermo-mechanical phenomena arising from the disposal of spent nuclear fuel, in: O. Stephansson, J.B. Hudson, L. Jing (Eds.), *Coupled Thermo-Hydro-Mechanical-Chemical Processes in Geosystems*, Elsevier, 2004.
- [11] Carnegie Mellon University web site, Triangle: A two-dimensional quality mesh generator and Delaunay triangulator. <http://www.cs.cmu.edu/quake/triangle.html>, 2007.
- [12] St. Cloud Zeolite Mining web site, What is zeolite? <http://www.stcloudmining.com/what-is-zeolite.html>, 2007.